

From independent patches to coordinated attention: Controlling information flow in vision transformers

Kieran A. Murphy¹

Abstract

We make the information transmitted by attention an explicit, measurable quantity in vision transformers. By inserting variational information bottlenecks on all attention-mediated writes to the residual stream—without other architectural changes—we train models with an explicit information cost and obtain a controllable spectrum from independent patch processing to fully expressive global attention. On ImageNet-100, we characterize how classification behavior and information routing evolve across this spectrum, and provide initial insights into how global visual representations emerge from local patch processing by analyzing the first attention heads that transmit information. By biasing learning toward solutions with constrained internal communication, our approach yields models that are more tractable for mechanistic analysis and more amenable to control.

1. Introduction

Transformers have emerged as a dominant architectural paradigm across machine learning, distinguished by their ability to aggregate information globally across the constitutive elements of an input (Vaswani et al., 2017). In vision transformers (Dosovitskiy et al., 2021), an image is decomposed into patches, and computation proceeds through repeated alternation between two modules: attention blocks, which enable information sharing across patches, and multi-layer perceptron (MLP) blocks, which refine patch representations independently. Because communication and local refinement occur in distinct computational steps, information flow becomes an explicit and manipulable axis of the architecture, rather than being inextricably entangled with processing as in prior paradigms. This naturally raises a mechanistic question: when communication is restricted, what

circuits of attention-mediated interaction emerge first (Olah et al., 2020; Elhage et al., 2021), and what do they reveal about how transformers build global understanding from local evidence?

Modern interpretability methods typically analyze models trained without any explicit pressure toward simplicity (Rudin, 2019; Samek et al., 2021) or prescribed explanatory structure (e.g., prototype-based or concept-bottleneck constraints) (Chen et al., 2019; Koh et al., 2020), often revealing internal mechanisms that are rich but difficult to disentangle or control. A complementary approach is to bias learning itself toward solutions with constrained information flow (Alemi et al., 2017). However, properly reasoning about the movement of information requires going beyond the deterministic, point-valued transformations that dominate standard architectures, which make it difficult to assign meaning to “information” in an operational sense (Saxe et al., 2019). One must instead introduce stochastic or probabilistic representations that allow information to be measured and restricted.

Such information-theoretic modifications to bottleneck the flow of information can be applied either post-hoc or during training. Post-hoc bottleneck methods (Schulz et al., 2020; Jiang et al., 2020; Hong et al., 2025) enable the study of pretrained models, but necessarily probe them under perturbations that differ from the conditions under which they were optimized, raising concerns about faithfulness. In contrast, training-time information restriction directly shapes the solutions that optimization discovers (Alemi et al., 2017; Achille & Soatto, 2018), yielding models whose internal computations are intrinsically biased toward limited communication. In this work, we pursue this second approach, using vision transformers as a natural setting in which to study restricted information routing in a clean and controlled way.

Our goal is a minimal modification to the transformer architecture that allows attention-mediated communication to be smoothly controlled, producing a spectrum of models that interpolates between fully expressive transformer computation and attention-less independent patch processing. We achieve this by inserting variational information bottlenecks on the writes to the residual stream performed by attention

¹Department of Computer Science, New Jersey Institute of Technology, Newark, NJ, USA 97102. Correspondence to: <kieran.murphy@njit.edu>.

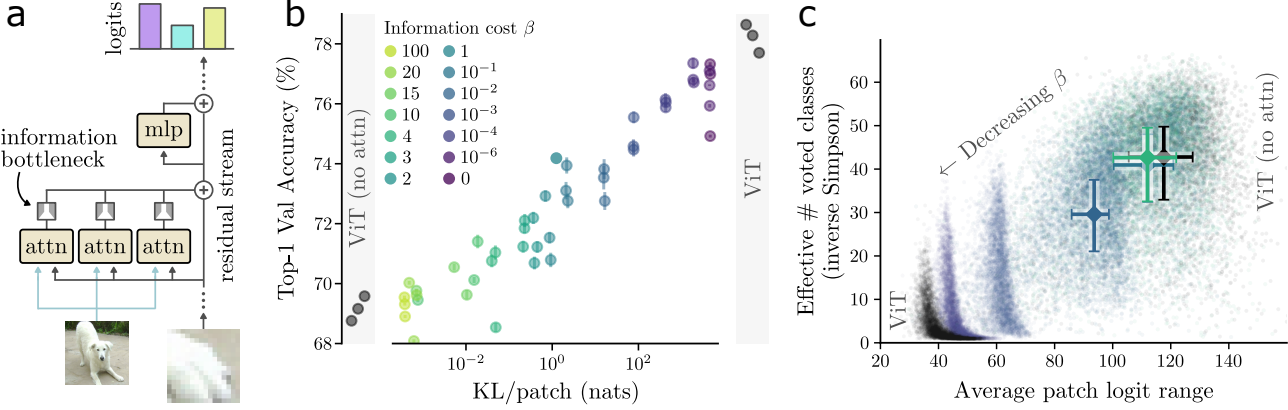


Figure 1. Limiting information written by attention to the residual stream. (a) We install an information bottleneck (IB) after every attention head and before anything is written to a patch’s residual stream. The sum total of information penalties is added to the original training loss, scaled by a parameter β that induces a spectrum from independent patch voting (no attention-mediated communication) to free-flowing information as in an unmodified ViT. (b) By installing IBs after each of the 36 attention heads in a ViT-tiny trained on a subset of Imagenet, we obtain a spectrum of models parameterized by the total amount of information written to the residual stream by attention heads. As the amount of information increases, so too does accuracy, smoothly covering the span between the ViT without attention (left) and the unmodified ViT (right). Error bars are shown only for the stochastic IB models (standard deviation across 10 validation runs). (c) The voting behavior of patches in a single image also smoothly interpolates between the two extremes as a function of β . We measure the average range of patch logits (min to max) and the variety of top-assigned classes across patches, using the inverse Simpson index as an effective count of diversity. Every dot represents an image from the dataset (colored by β with the same mapping as in b), and the median with interquartile ranges is shown for the point clouds with significant overlap.

blocks, without otherwise altering the attention mechanism or transformer structure. This yields a family of models in which communication capacity becomes a tunable parameter.

At the zero-communication limit, the architecture reduces to independent per-patch processing followed by permutation-invariant aggregation, closely related to the DeepSets formulation (Zaheer et al., 2017). This provides a well-defined and interpretable endpoint. As communication capacity increases, global visual representations emerge progressively from local patch computations. By analyzing performance, patch-level information updates, and the first attention heads that become active, we obtain a mechanistic picture of how transformers begin to integrate information across space under constrained bandwidth.

Contributions. Concretely, we: (i) introduce a controllable family of vision transformers with variational bottlenecks on every attention-mediated write to the residual stream; (ii) characterize the tradeoff between accuracy and routed information across a spectrum from independent patch processing to standard ViTs on ImageNet-100; and (iii) provide a fine-grained analysis of the first attention heads that transmit information, illustrating how global computation emerges from restricted local processing. Overall, our results suggest that training-time information restriction yields models that are intrinsically more interpretable and

more amenable to analysis and control.

2. Related work

Mechanistic interpretability and transformer circuits. The aim of this work aligns with mechanistic interpretability: to understand and ultimately control the internal information processing of transformer models. Two complementary directions have emerged in this literature. The first traces the flow of information between sequence elements as mediated by attention, identifying structured computational subgraphs or “circuits” within trained networks (Olah et al., 2020; Elhage et al., 2021). The second seeks to decompose high-dimensional representation spaces into more interpretable features or concepts, for example through sparse dictionary learning or superposition-based analyses (Bricken et al., 2023; Huben et al., 2024). Because full-scale models are challenging to analyze directly, many mechanistic insights have been developed in simplified settings, including small or partially linearized transformers (Elhage et al., 2021) and narrowly defined tasks (Akyürek et al., 2023; Nanda et al., 2023; Wang et al., 2023; Dutta et al., 2024). Our work contributes a complementary form of simplification: rather than restricting model size or task complexity, we restrict internal communication capacity during training, yielding a controllable spectrum of transformer computations.

Mechanistic interpretability beyond language. Most mechanistic interpretability research has focused on autoregressive language models, where attention patterns and discrete token structure provide a natural substrate for circuit analysis. Extending these ideas to vision transformers is less mature: sequence elements correspond to continuous image patches rather than symbols, attention is typically dense rather than masked, and the relevant computations are harder to localize in semantic units. Nevertheless, several lines of work have begun to probe the internal organization of ViTs, including representation-level studies of how transformer features evolve with depth and differ from CNNs (Raghu et al., 2021; Caron et al., 2021; Park et al., 2023; Dorszewski et al., 2026), and feature-decomposition approaches such as sparse autoencoders applied to ViT activations (Stevens et al., 2025). These differ from attribution-based explainability methods (Chefer et al., 2021; Covert et al., 2023; Achitabat et al., 2024) in that they aim to characterize internal representations, but they still analyze models after training rather than shaping information flow during learning. In contrast, we study how global visual representations emerge from local patch processing when attention-mediated communication is explicitly restricted during optimization.

Information bottleneck methods for interpretability. The methodology of this work is closely related to the information bottleneck principle (Tishby et al., 2000; Alemi et al., 2017), which formalizes learning as a tradeoff between predictive sufficiency and compression. While the information bottleneck has been widely used as a regularizer or robustness tool (Hu et al., 2024), a distinct line of work uses bottlenecks to reveal which information is most important to a model’s computation. Several approaches apply information bottlenecks post-hoc to pretrained networks, including the Information Bottleneck Attribution method (IBA) (Schulz et al., 2020) and subsequent extensions (Jiang et al., 2020; Hong et al., 2025). Other approaches incorporate bottlenecks directly during training, enabling analysis in the same regime in which the model was optimized. For example, distributed information bottleneck methods have been used to quantify feature importance by restricting communication about input dimensions in tabular settings (Murphy & Bassett, 2023; 2024). Our work extends this training-time bottleneck perspective to the internal communication pathways of transformers by placing variational bottlenecks on attention-mediated residual writes.

Communication restriction and structured simplification in transformers. A closely related set of ideas seeks to simplify transformer computation by limiting or pruning attention and token interactions. Prior work has explored attention head pruning and sparsification (Michel et al., 2019; Voita et al., 2019), as well as token pruning and adaptive computation in vision transformers (Pan et al., 2021; Rao

et al., 2021; Liang et al., 2022). These approaches primarily aim to improve efficiency, whereas our goal is interpretability: by making communication costly during training, we obtain a spectrum from independent patch processing to fully expressive attention, and can analyze which attention heads and latent dimensions first become active as capacity increases.



Figure 2. KL allocation across patches. For a random sample of validation images that ViT correctly classified, we show the total KL per patch (summed across all attention heads in the model) for a selection of models nearest to the Pareto front in Fig. 1. Note that the colormaps have the same range for each model (column).

3. Method

We begin with a brief review of the vision transformer architecture, then introduce our training-time information restriction mechanism, and finally describe how we characterize the resulting spectrum of information routing behaviors.

3.1. Vision transformers as residual stream communication

We adopt the residual stream framing of transformer computation developed in Elhage et al. (2021). A vision transformer (ViT) processes an image as a sequence of patch embeddings, $\mathcal{S} = \{x_i\}_{i=1}^N$, where each patch maintains

its own residual stream representation throughout the network. Each transformer block alternates between two update mechanisms: (i) an attention block, which computes context-dependent interactions across patches, and (ii) an MLP block, which refines each patch representation independently.

Crucially, only attention enables information exchange between sequence elements (Fig. 1a). MLP blocks operate pointwise on each residual stream and introduce no new cross-patch information. Thus, attention-mediated writes to the residual stream constitute the natural pathway through which global visual representations emerge from local patch features. Our approach directly monitors and restricts this communication channel.

3.2. Bottlenecking attention-mediated residual writes

Within an attention block, there are multiple possible intervention points at which one could restrict information flow. We choose the final attention update immediately before it is written back into the residual stream. This placement leaves the attention computation itself intact, while controlling the amount of information that can be transmitted through the update. To obtain head-resolved control over communication, we instantiate a separate variational bottleneck on every attention head in every layer (36 bottlenecks total in ViT-Tiny), so that each head constitutes an independently regularized information channel.

Concretely, let $\Delta_i^\ell \in \mathbb{R}^d$ denote the attention update for patch i at layer ℓ prior to the output projection. In a standard transformer block, this update is added deterministically to the residual stream. Instead, we route Δ_i^ℓ through a variational information bottleneck:

$$\Delta_i^\ell \rightarrow z_i^\ell \sim q_\phi(z | \Delta_i^\ell) \rightarrow \hat{\Delta}_i^\ell = g_\theta(z_i^\ell), \quad (1)$$

where q_ϕ is an encoder network producing a stochastic latent representation, and g_θ is a decoder mapping back to the original update space. The decoded update $\hat{\Delta}_i^\ell$ is then projected and written to the residual stream as usual. By intervening only at the attention-mediated residual write—the sole mechanism by which patches exchange information—we obtain a deliberately minimal modification that isolates inter-patch communication without otherwise altering ViT computation. This targeted design yields a controlled and interpretable axis of variation in global information routing.

3.3. Training objective and information restriction

Our bottlenecks are trained using the variational information bottleneck (VIB) principle (Tishby et al., 2000; Alemi et al., 2017). Each latent variable is modeled as a diagonal Gaussian,

$$q_\phi(z | \Delta) = \mathcal{N}(\mu_\phi(\Delta), \text{diag}(\sigma_\phi^2(\Delta))), \quad (2)$$

and is regularized toward an isotropic unit Gaussian prior $p(z) = \mathcal{N}(0, I)$. The resulting KL divergence upper bounds the mutual information between Δ and z , yielding a tractable measure of transmitted information.

We train the model with the objective

$$\mathcal{L} = \mathcal{L}_{\text{cls}} + \beta \sum_{\ell, i} \mathbb{E}_{q_\phi(z_i^\ell | \Delta_i^\ell)} [D_{\text{KL}}(q_\phi(z_i^\ell | \Delta_i^\ell) \| p(z))], \quad (3)$$

where \mathcal{L}_{cls} is the standard cross-entropy loss and β controls the strength of the information restriction. Varying β therefore provides a single, interpretable control knob that continuously tunes the capacity of the network’s communication channel, from independent patch processing to the fully expressive ViT.

Although applying bottlenecks simultaneously across many layers departs from the classical single-bottleneck IB formulation, it provides a principled restriction on the total *variety* of attention-mediated updates that can be transmitted through the network. Moreover, the resulting IB latent spaces admit rich information-theoretic and mechanistic analyses.

Comparing probabilistic head updates via normalized mutual information. To compare the information content of two attention-head bottlenecks, we treat each head as inducing a soft clustering assignment over patches (Murphy et al., 2025). For a given head, let X denote the discrete patch identity (indexed over all patches in the validation set) and let U denote the corresponding bottleneck latent variable. Each head therefore defines a stochastic channel $p(u|x)$ through its variational posterior.

We estimate the mutual information between patch identities and latent messages using a Monte Carlo approximation based on the aggregated posterior over a dataset of size L :

$$I(X; U) = \mathbb{E}_{x \sim p(x)} \mathbb{E}_{u \sim p(u|x)} \left[\log \frac{p(u|x)}{\frac{1}{L} \sum_i^L p(u|x_i)} \right], \quad (4)$$

where the denominator provides an empirical estimate of the marginal $p(u)$.

To quantify the correspondence between two heads with latent variables U and V , we form a joint channel by concatenating their distributional parameters, yielding samples from $p(u, v | x)$. Using the identity

$$I(U; V) = I(X; U) + I(X; V) - I(X; U, V), \quad (5)$$

we obtain an estimate of the shared information between headwise messages. Finally, we report a normalized mutual information,

$$\text{NMI}(U, V) = \frac{I(U; V)}{\sqrt{I(U; U') I(V; V')}}, \quad (6)$$

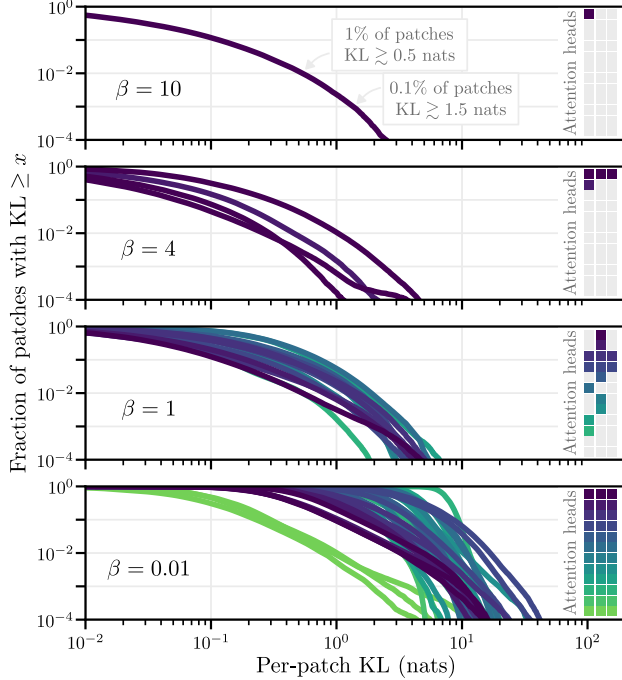


Figure 3. Attention head firing patterns. Survival function $P(KL \geq x)$ of per-patch information across attention heads, showing that only a small fraction of patches carry significant routed information in the high- β regime. The grids on the right show which heads are active, starting with block 0 at the bottom.

where U' and V' denote independent samples from the same headwise channels. Uncertainty is propagated from the standard error of the Monte Carlo estimates of $I(X; U)$.

3.4. Implementation details

All experiments use the ViT-Tiny backbone from `timm` (12 blocks, embedding dimension 192, 3 attention heads per block). We adopt this lightweight backbone to enable extensive sweeps over information budgets and detailed mechanistic analysis, while preserving the canonical transformer computation pattern. We insert variational information bottlenecks on the attention-mediated residual writes in every block, instantiating a separate encoder-decoder bottleneck for each head in each layer (36 bottlenecks total). This design treats each head as an independently regularized communication channel while leaving the remainder of the ViT computation unchanged. All bottlenecks share the same architecture and latent dimensionality, differing only in their learned parameters.

For classification, we employ global average pooling over patch representations followed by the standard linear classifier head (Zhai et al., 2022), ensuring that the zero-communication limit remains well-defined.

We train models on the ImageNet-100 subset introduced

by Tian et al. (2020), using AdamW with learning rate 6×10^{-4} and weight decay 0.05 for 1000 epochs. Training uses a cosine learning-rate schedule with 10 epochs of warmup, and the information penalty coefficient β is fixed over the course of training. We apply RandAugment for standard appearance-level augmentation, but omit patch-mixing strategies such as Mixup and CutMix since these distort patch-level statistics and complicate interpretation. Additional optimization and augmentation details are provided in Appendix A.

4. Results

We present results at two complementary scales. First, we characterize the continuum of models induced by the information cost β , demonstrating systematic changes in attention-mediated communication, predictive performance, and patch-based voting behavior. Second, we exploit the sparsity of the low-information regime to perform fine-grained mechanistic analyses of individual attention heads.

4.1. Properties of the spectrum of models

The entire spectrum from independent patch processing (attention blocks are removed from the ViT) to freely flowing information as in an unmodified ViT, spans $69.2\% \pm 0.3$ to $78.2\% \pm 0.3$ top-1 validation accuracy (mean and standard deviation over three random seeds) (Fig. 1b). That the attention-less baseline remains competitive underscores that substantial visual recognition can be achieved from simple pooling of local patch evidence alone, consistent with the strong performance of local-feature-based image representations prior to deep networks (Lowe, 2004; Sánchez et al., 2013).

Intuitively, as information communicated by attention increases, so too does classification performance. With only around one nat of KL for every ten patches, accuracy increases by 1 – 2%. When around one nat of KL is communicated per patch, it further increases by $\sim 2\%$. Empirically, accuracy increases approximately linearly with $\log KL$ over much of the spectrum. The least restricted models ($\beta = 0$) approach, though do not fully reach, the accuracy of an unmodified ViT (within $\sim 1\%$ top-1), suggesting a small residual effect of the IB parameterization even in the weakly constrained regime.

Without attention to pass information between patches, there can clearly be no consensus between patch representations. How does patch independence give way to consensus as attention becomes less restricted? We show in Fig. 1c characteristics of patch voting behaviors for several models close to the Pareto front. These patch-level measures provide a complementary view of global integration: rather than only tracking top-1 accuracy, they quantify how communication

induces consensus among local predictions. The spectrum therefore captures not just performance gains, but a qualitative transition from diverse independent patch hypotheses to coordinated global representations.

First, we characterize the variety of top-class assignments by patch, using the inverted Simpson index as an effective count of the number of classes (Simpson, 1949; Hill, 1973). The inverted Simpson index, $1 / \sum_c p_c^2$ with p_c the fraction of patches with top-assigned class c , provides an effective number of distinct classes represented in the patch-level votes. Second, we evaluate the total range of patch logit contributions, from min to max, as a form of opinionation of the patches comprising an image. Independent patch processing yields a large variety of output class assignments (effective counts often exceeding 50 different classes per image) and more significant opinionation (total logit range $\gtrsim 100$) than the unmodified ViT. Importantly, we are able to smoothly and controllably interpolate between these extremes by tuning the information cost coefficient β .

We visualize aspects of the processing of a handful of images by different models in Fig 2 and in Appx. C. For the IB models, we display a heatmap of the information penalty (in terms of KL divergence) summed across all attention heads for each patch in the image. Because each bottleneck yields a per-patch KL cost, we obtain a direct, quantitative map of where attention allocates its limited communication budget. As is perhaps intuitive from the relatively small performance gap between independent patch processing and the full ViT (Fig. 1b), there is high agreement of classification probability vectors along the full spectrum for the majority of images (Appx. B). We therefore focus on images from the validation set for which ViT (unmodified) and ViT (w/o attn) vary the most in the final classification. Specifically, we compute the Jensen-Shannon distance between the probability vectors output by the two models for a given image (Lin, 2002), and randomly sample from the top 10% of images. This focuses attention on cases where global communication most strongly alters the prediction, while avoiding cherry-picking individual examples. In Appx. C, we show samples based on other criteria (e.g., misclassified by ViT) and additionally visualize examples of patch voting behavior.

4.2. Update behavior of individual attention heads

What is the contextual information required for maximal performance, that the independent patch processing cannot access? To answer this requires interpreting the information content of the updates to the residual stream.

A striking consequence of the information penalty is that many headwise channels collapse to the prior, yielding near-zero KL and effectively inactive heads. This sparsity substantially simplifies mechanistic analysis in the low-

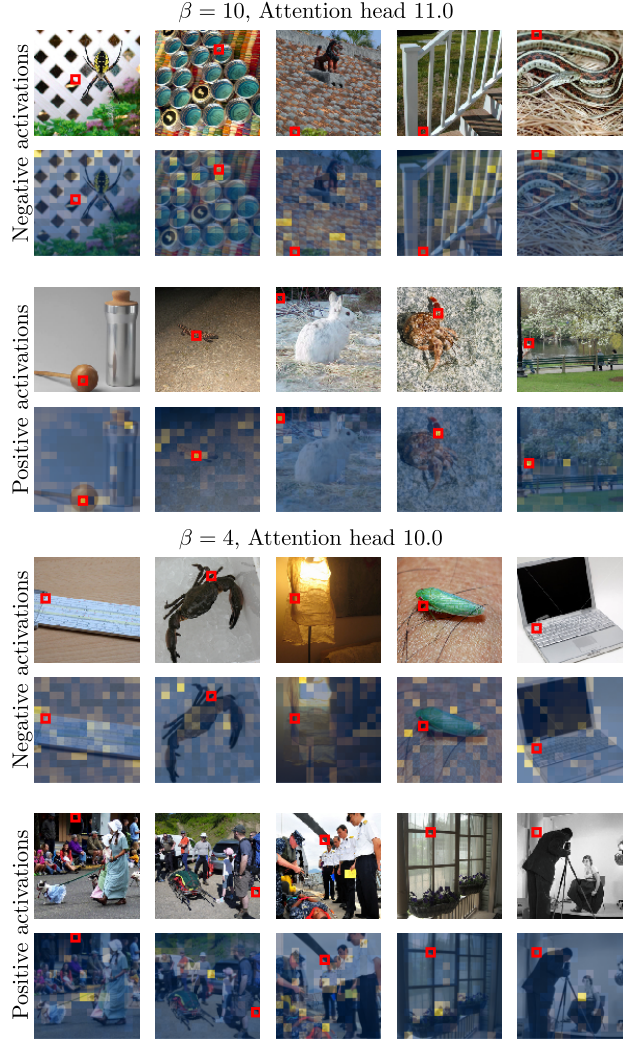


Figure 4. Extreme activating patches. For the single active attention head in the $\beta = 10$ model (head 11.0), and for one of the four effectual heads of the $\beta = 4$ model (head 10.0), we randomly sample positive and negative activations from patches in the top 0.1% of KL cost. The patch is indicated by a red square in both the original image (top of each pair of rows) and the head’s attention map (bottom of each pair of rows).

information regime. We show in Fig. 3 the survival function $\Pr(\text{KL} \geq x)$ of per-patch information for all patches in the validation set and for all heads. We deem a head active if its KL exceeds 10^{-2} nats for at least one patch in the validation set. Only one attention head is ‘active’ at $\beta = 10$, and four heads are active for the $\beta = 4$ model. The heads that are active spend KL sparingly: 99% of patches receive an update costing less than 0.5 nats in the $\beta = 10$ case. For the low-information models ($\beta = 10, 4, 1$), the behavior is the same across heads, where the majority of patches get the same null update and the representation nearly mirrors the prior of the channel. As the information restriction loosens,

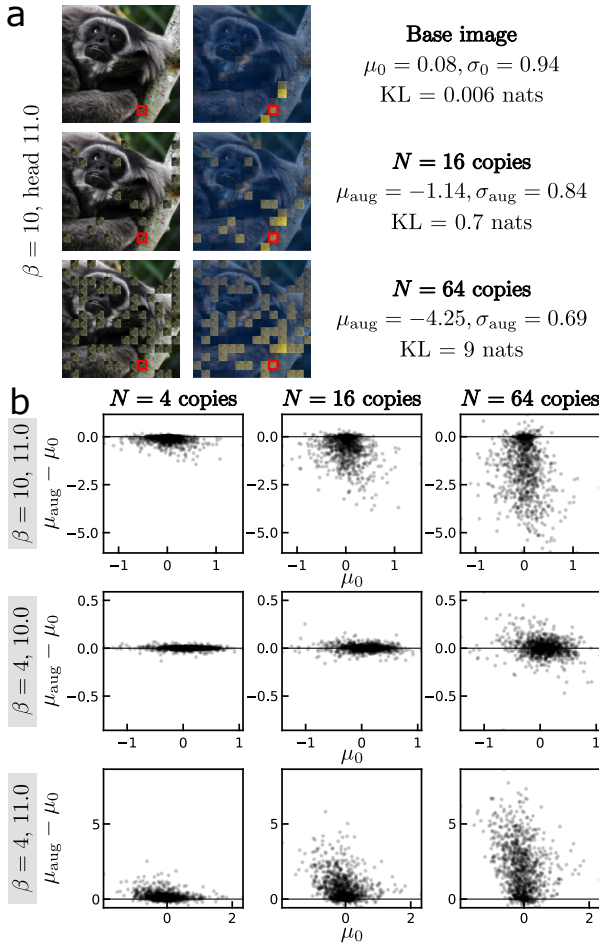


Figure 5. Probing the repetition hypothesis. (a) Given a patch and a base image, we randomly copy the given patch to N other locations in the image before passing the augmented image through the model. For head 11.0 of the $\beta = 10$ model, the repetition of the patch systematically drives the attention head’s update representation to larger negative values. The corresponding attention maps highlight the copy locations. (b) A random selection of 1024 patches in the dataset was augmented with patch copies as in a, at three different magnitudes and for three different attention heads (from the $\beta = 10$ and $\beta = 4$ models). We display the base image’s representation mean, μ_0 , and the signed displacement in representation space, $\mu_{\text{aug}} - \mu_0$, caused by the augmentation.

$\beta = 0.01$ utilizes all 36 attention heads for non-trivial updates, and the distribution of KLS spent per patch shifts significantly, to where the majority deviate from the prior.

Moreover, active heads often use only one or two latent dimensions in the low-information regime, enabling especially direct visualization of update directionality. When the latent is effectively one-dimensional, the update reduces to a signed scalar message, allowing patches to be grouped by whether the head transmits a positive or negative signal. In Fig. 4 we show high-update patches for the single

active attention head in the $\beta = 10$ model as well as the corresponding attention maps. Examples for other attention heads can be found in Appendix D.

The first attention head to turn on—the attention-mediated updates that are worth paying a steep information cost—appear to encode coarse statistics of patch similarity elsewhere in the image, effectively updating patches with a tag that they are part of a repeated pattern, as suggested by the negatively activating examples in Fig. 4 for $\beta = 10$, head 11.0. Across three random seeds, all $\beta = 10$ models contain an active head that appears to activate on repetition (Appx. D). This suggests that coarse redundancy or similarity signals are among the most information-efficient messages to transmit: they are cheap to communicate, yet provide useful global context early in the spectrum.

We test this hypothesis through augmentations that change the relationship between highly activating patches and their containing image (Fig. 5). For a random sample of 1024 images, and within each a randomly selected patch, we apply a stochastic augmentation that copy-pastes the selected patch multiple times elsewhere in the image. This manipulation increases within-image redundancy while preserving local patch content. The effect is pronounced for the heads that seem to detect repetition: as the number of copy-pastes grows from 4 to 16 and then to 64, the mean of the latent distribution (representing the content of the attention-mediated update) continues to shift a larger amount, consistently across diverse starting patches. This is clear for $\beta = 10$ head 11.0 and $\beta = 4$ head 11.0, whereas no such systematic effect is seen for $\beta = 4$ head 10.0.

As communication capacity increases, attention heads diversify in function, making single-head interpretation more nuanced. Controlled perturbations therefore play a central role in grounding mechanistic hypotheses about the messages each head transmits. In the case of head 11.0 of $\beta = 10$, the perturbations provide convergent evidence for repetition-sensitive messaging. We next compare the information content of the attention head updates across models with different information costs and across models with different seeds. Note that the probabilistic nature of the attention head updates renders prevalent point-based representation similarity measures (e.g., (Kornblith et al., 2019; Klabunde et al., 2025)) problematic. We employ recently a proposed measure that generalizes normalized mutual information (NMI) as a comparison between hard clustering assignments to be applicable to probabilistic representation spaces (Murphy et al., 2025). We interpret each head’s updates as inducing a soft clustering over patches conditioned on image context, and then compare the information content of the soft clustering assignments.

In Fig. 6 we show the pairwise NMI between heads of various models. For reference, NMI ranges from zero (no

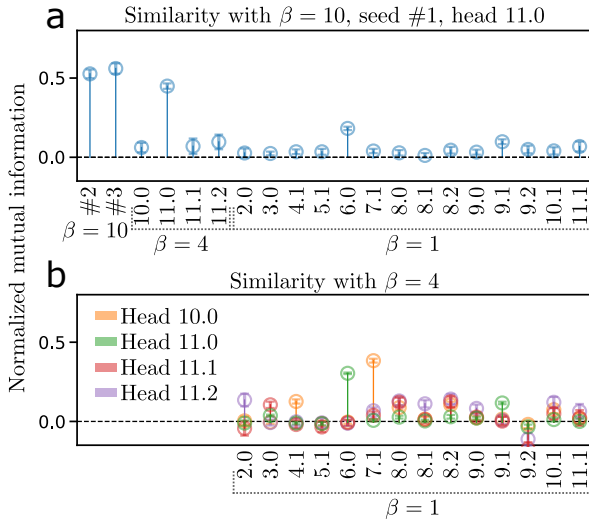


Figure 6. Measuring the similarity of attention heads. (a) For $\beta = 10$ head 11.0, we evaluate pairwise similarity with two other models trained at $\beta = 10$ with different random seeds (labeled #2 and #3), with the four active heads in the $\beta = 4$ model, and the 14 active heads in the $\beta = 1$ model. The Monte Carlo estimate for mutual information described in the main text was sampled with 2×10^7 samples; error bars show propagated uncertainty on NMI. (b) The four heads of the $\beta = 4$ model were each compared to all of the heads of the $\beta = 1$ model.

shared information) to one (identical treatment of the entire dataset). Across three repeats with different random seeds, the active heads of the $\beta = 10$ models have high agreement, indicating a robustness of the particular tagging information seen in Fig. 4. Further, the information tagged by the attention heads of $\beta = 10$ is seen again, to a lesser degree, in the models trained with $\beta = 4$ (head 11.0) and $\beta = 1$ (head 6.0). The (dis)similarity of behavior under the copy-paste augmentations in Fig. 5 is seen in the corresponding NMI values: high for head 11.0 and low for head 10.0 of the $\beta = 4$ model. When comparing the $\beta = 4$ model's, four active heads to the $\beta = 1$ model's fourteen active heads, there are few strong similarities worthy of deeper comparison.

Importantly, while granular inspection of a single head is greatly aided by posterior collapse down to a single dimension, the normalized mutual information comparison is agnostic to the dimensionalities of the latent spaces (Murphy et al., 2025). This provides a practical route for scaling mechanistic insights from highly constrained, low-dimensional channels to richer models further along the spectrum.

5. Discussion

Scalability remains a central challenge for mechanistic interpretability. Even in the most constrained regime, we in-

terpret models with only a handful of active attention heads transmitting fractions of a bit per image. Yet a wide gap remains between these sparse, low-bandwidth circuits and the dense communication patterns of models approaching the performance of an unrestricted ViT (Fig. 1b). Understanding how distributed attention-based computation emerges as information constraints relax will be essential for scaling interpretability beyond highly simplified settings.

A key contribution of this work is to make attention an explicit, measurable communication channel. By placing variational bottlenecks directly on attention-mediated residual writes, we obtain a controlled spectrum from independent patch processing to fully expressive global attention, without otherwise modifying transformer computation (Fig. 1a). This provides a principled axis of simplification: rather than reducing model size or restricting to synthetic tasks, we restrict internal communication capacity itself. We view this spectrum as a laboratory for tracing how attention circuits emerge as bandwidth increases.

Our results suggest that the earliest attention circuits to emerge under strong information restriction implement coarse but high-value forms of global integration. Across seeds, the first active heads consistently appear sensitive to patch repetition or redundancy (Figs. 4, 5), indicating that such global texture statistics may be among the most information-efficient computations available to the model.

Several aspects of the intermediate regimes depend on modeling choices. Our bottlenecks use Gaussian posteriors and KL regularization, and global average pooling provides a particularly clean zero-communication limit. Extending this framework to larger backbones, alternative aggregation structures, and richer datasets will be important for assessing the generality of the emergent behaviors we observe.

Finally, training a separate model for each information budget is computationally expensive. However, once trained, each point in the spectrum provides a stable object for mechanistic investigation, yielding models whose internal communication is intrinsically constrained and whose active heads are sparse and tractable. We view such information-restricted transformers as a useful laboratory for studying how global visual computation emerges from local processing under limited bandwidth.

Impact Statement

This paper presents work whose goal is to advance the field of Machine Learning. There are many potential societal consequences of our work, none of which we feel must be specifically highlighted here.

Acknowledgments

We thank Thanh Nguyen for helpful feedback on the manuscript.

References

Achille, A. and Soatto, S. Information dropout: Learning optimal representations through noisy computation. *IEEE Transactions on Pattern Analysis and Machine Intelligence*, 40(12):2897–2905, 2018.

Achitbat, R., Hatefi, S. M. V., Dreyer, M., Jain, A., Wiegand, T., Lapuschkin, S., and Samek, W. AttnLRP: Attention-aware layer-wise relevance propagation for transformers. In Salakhutdinov, R., Kolter, Z., Heller, K., Weller, A., Oliver, N., Scarlett, J., and Berkenkamp, F. (eds.), *Proceedings of the 41st International Conference on Machine Learning*, volume 235 of *Proceedings of Machine Learning Research*, pp. 135–168. PMLR, 21–27 Jul 2024.

Akyürek, E., Schuurmans, D., Andreas, J., Ma, T., and Zhou, D. What learning algorithm is in-context learning? investigations with linear models. In *The Eleventh International Conference on Learning Representations*, 2023. URL <https://openreview.net/forum?id=0g0X4H8yN4I>.

Alemi, A. A., Fischer, I., Dillon, J. V., and Murphy, K. Deep variational information bottleneck. In *International Conference on Learning Representations*, 2017. URL <https://openreview.net/forum?id=HyxQzBceg>.

Bricken, T., Templeton, A., Batson, J., Chen, B., Jermyn, A., Conerly, T., Turner, N., Anil, C., Denison, C., Askell, A., Lasenby, R., Wu, Y., Kravec, S., Schiefer, N., Maxwell, T., Joseph, N., Hatfield-Dodds, Z., Tamkin, A., Nguyen, K., McLean, B., Burke, J. E., Hume, T., Carter, S., Henighan, T., and Olah, C. Towards monosemanticity: Decomposing language models with dictionary learning. *Transformer Circuits Thread*, 2023. <https://transformercircuits.pub/2023/monosemantic-features/index.html>.

Caron, M., Touvron, H., Misra, I., Jégou, H., Mairal, J., Bojanowski, P., and Joulin, A. Emerging properties in self-supervised vision transformers. In *Proceedings of the IEEE/CVF international conference on computer vision*, pp. 9650–9660, 2021.

Chefer, H., Gur, S., and Wolf, L. Transformer interpretability beyond attention visualization. In *Proceedings of the IEEE/CVF conference on computer vision and pattern recognition*, pp. 782–791, 2021.

Chen, C., Li, O., Tao, D., Barnett, A., Rudin, C., and Su, J. K. This looks like that: deep learning for interpretable image recognition. *Advances in neural information processing systems*, 32, 2019.

Covert, I. C., Kim, C., and Lee, S.-I. Learning to estimate shapley values with vision transformers. In *The Eleventh International Conference on Learning Representations*, 2023. URL https://openreview.net/forum?id=5ktFNz_pJLK.

Cubuk, E. D., Zoph, B., Shlens, J., and Le, Q. Randaugment: Practical automated data augmentation with a reduced search space. In Larochelle, H., Ranzato, M., Hadsell, R., Balcan, M., and Lin, H. (eds.), *Advances in Neural Information Processing Systems*, volume 33, pp. 18613–18624. Curran Associates, Inc., 2020. URL https://proceedings.neurips.cc/paper_files/paper/2020/file/d85b63ef0ccb114d0a3bb7b7d808028f-Paper.pdf.

Dorszewski, T., Tětková, L., Jenssen, R., Hansen, L. K., and Wickstrøm, K. K. From colors to classes: Emergence of concepts in vision transformers. In Guidotti, R., Schmid, U., and Longo, L. (eds.), *Explainable Artificial Intelligence*, pp. 28–47. Springer Nature Switzerland, 2026.

Dosovitskiy, A., Beyer, L., Kolesnikov, A., Weissenborn, D., Zhai, X., Unterthiner, T., Dehghani, M., Minderer, M., Heigold, G., Gelly, S., Uszkoreit, J., and Houlsby, N. An image is worth 16x16 words: Transformers for image recognition at scale. In *International Conference on Learning Representations*, 2021. URL <https://openreview.net/forum?id=YicbFdNTTy>.

Dutta, S., Singh, J., Chakrabarti, S., and Chakraborty, T. How to think step-by-step: A mechanistic understanding of chain-of-thought reasoning. *Transactions on Machine Learning Research*, 2024. ISSN 2835-8856. URL <https://openreview.net/forum?id=uHLDkQVtyC>.

Elhage, N., Nanda, N., Olsson, C., Henighan, T., Joseph, N., Mann, B., Askell, A., Bai, Y., Chen, A., Conerly, T., DasSarma, N., Drain, D., Ganguli, D., Hatfield-Dodds, Z., Hernandez, D., Jones, A., Kernion, J., Lovitt, L., Ndousse, K., Amodei, D., Brown, T., Clark, J., Kaplan, J., McCandlish, S., and Olah, C. A mathematical framework for transformer circuits. *Transformer Circuits Thread*, 2021. <https://transformercircuits.pub/2021/framework/index.html>.

Hill, M. O. Diversity and evenness: a unifying notation and its consequences. *Ecology*, 54(2):427–432, 1973.

Hong, J.-H., Kim, H.-J., Jeon, K.-S., and Lee, S.-W. Comprehensive information bottleneck for unveiling universal attribution to interpret vision transformers. In 2025

IEEE/CVF Conference on Computer Vision and Pattern Recognition (CVPR), pp. 25166–25175, 2025. doi: 10.1109/CVPR52734.2025.02343.

Hu, S., Lou, Z., Yan, X., and Ye, Y. A survey on information bottleneck. *IEEE Transactions on Pattern Analysis and Machine Intelligence*, 46(8):5325–5344, 2024.

Huben, R., Cunningham, H., Smith, L. R., Ewart, A., and Sharkey, L. Sparse autoencoders find highly interpretable features in language models. In *The Twelfth International Conference on Learning Representations*, 2024. URL <https://openreview.net/forum?id=F76bwRSLeK>.

Jiang, Z., Tang, R., Xin, J., and Lin, J. Inserting Information Bottlenecks for Attribution in Transformers. In *Findings of the Association for Computational Linguistics: EMNLP 2020*, pp. 3850–3857, Online, November 2020. Association for Computational Linguistics. URL <https://www.aclweb.org/anthology/2020.findings-emnlp.343>.

Klabunde, M., Schumacher, T., Strohmaier, M., and Lemmerich, F. Similarity of neural network models: A survey of functional and representational measures. *ACM Computing Surveys*, 57(9):1–52, 2025.

Koh, P. W., Nguyen, T., Tang, Y. S., Mussmann, S., Pierson, E., Kim, B., and Liang, P. Concept bottleneck models. In *International conference on machine learning*, pp. 5338–5348. PMLR, 2020.

Kornblith, S., Norouzi, M., Lee, H., and Hinton, G. Similarity of neural network representations revisited. In *International conference on machine learning*, pp. 3519–3529. PMLR, 2019.

Liang, Y., Ge, C., Tong, Z., Song, Y., Wang, J., and Xie, P. Not all patches are what you need: Expediting vision transformers via token reorganizations. *arXiv preprint arXiv:2202.07800*, 2022.

Lin, J. Divergence measures based on the shannon entropy. *IEEE Transactions on Information theory*, 37(1):145–151, 2002.

Lowe, D. G. Distinctive image features from scale-invariant keypoints. *International journal of computer vision*, 60(2):91–110, 2004.

Michel, P., Levy, O., and Neubig, G. Are sixteen heads really better than one? *Advances in neural information processing systems*, 32, 2019.

Murphy, K. A. and Bassett, D. S. Interpretability with full complexity by constraining feature information. In *International Conference on Learning Representations (ICLR)*, 2023. URL https://openreview.net/forum?id=R_OL5mLhsv.

Murphy, K. A. and Bassett, D. S. Information decomposition in complex systems via machine learning. *Proceedings of the National Academy of Sciences*, 121(13):e2312988121, 2024.

Murphy, K. A., Dillavou, S., and Bassett, D. S. Comparing the information content of probabilistic representation spaces. *Transactions on Machine Learning Research*, 2025. ISSN 2835-8856. URL <https://openreview.net/forum?id=adhsMqURI1>.

Nanda, N., Chan, L., Lieberum, T., Smith, J., and Steinhardt, J. Progress measures for grokking via mechanistic interpretability. In *The Eleventh International Conference on Learning Representations*, 2023. URL <https://openreview.net/forum?id=9XF5bDPmdW>.

Olah, C., Cammarata, N., Schubert, L., Goh, G., Petrov, M., and Carter, S. Zoom in: An introduction to circuits. *Distill*, 5(3):e00024–001, 2020.

Pan, B., Panda, R., Jiang, Y., Wang, Z., Feris, R., and Oliva, A. Ia-red²: Interpretability-aware redundancy reduction for vision transformers. *Advances in neural information processing systems*, 34:24898–24911, 2021.

Park, N., Kim, W., Heo, B., Kim, T., and Yun, S. What do self-supervised vision transformers learn? In *The Eleventh International Conference on Learning Representations*, 2023. URL <https://openreview.net/forum?id=azCKuYyS74>.

Raghu, M., Unterthiner, T., Kornblith, S., Zhang, C., and Dosovitskiy, A. Do vision transformers see like convolutional neural networks? *Advances in neural information processing systems*, 34:12116–12128, 2021.

Rao, Y., Zhao, W., Liu, B., Lu, J., Zhou, J., and Hsieh, C.-J. Dynamiccvit: Efficient vision transformers with dynamic token sparsification. *Advances in neural information processing systems*, 34:13937–13949, 2021.

Rudin, C. Stop explaining black box machine learning models for high stakes decisions and use interpretable models instead. *Nature Machine Intelligence*, 1(5):206–215, 2019.

Samek, W., Montavon, G., Lapuschkin, S., Anders, C. J., and Müller, K.-R. Explaining deep neural networks and beyond: A review of methods and applications. *Proceedings of the IEEE*, 109(3):247–278, 2021.

Sánchez, J., Perronnin, F., Mensink, T., and Verbeek, J. Image classification with the fisher vector: Theory and practice. *International journal of computer vision*, 105(3):222–245, 2013.

Saxe, A. M., Bansal, Y., Dapello, J., Advani, M., Kolchinsky, A., Tracey, B. D., and Cox, D. D. On the information bottleneck theory of deep learning. *Journal of Statistical Mechanics: Theory and Experiment*, 2019(12):124020, dec 2019. doi: 10.1088/1742-5468/ab3985. URL <https://doi.org/10.1088%2F1742-5468%2Fab3985>.

Schulz, K., Sixt, L., Tombari, F., and Landgraf, T. Restricting the flow: Information bottlenecks for attribution. In *International Conference on Learning Representations*, 2020. URL <https://openreview.net/forum?id=S1xWh1rYwB>.

Simpson, E. H. Measurement of diversity. *nature*, 163 (4148):688–688, 1949.

Stevens, S., Chao, W.-L., Berger-Wolf, T., and Su, Y. Sparse autoencoders for scientifically rigorous interpretation of vision models. *arXiv preprint arXiv:2502.06755*, 2025.

Tian, Y., Krishnan, D., and Isola, P. Contrastive multiview coding. In Vedaldi, A., Bischof, H., Brox, T., and Frahm, J.-M. (eds.), *Computer Vision – ECCV 2020*, pp. 776–794, Cham, 2020. Springer International Publishing. ISBN 978-3-030-58621-8.

Tishby, N., Pereira, F. C., and Bialek, W. The information bottleneck method. *arXiv preprint physics/0004057*, 2000.

Vaswani, A., Shazeer, N., Parmar, N., Uszkoreit, J., Jones, L., Gomez, A. N., Kaiser, L., and Polosukhin, I. Attention is all you need. *Advances in neural information processing systems*, 30, 2017.

Voita, E., Talbot, D., Moiseev, F., Sennrich, R., and Titov, I. Analyzing multi-head self-attention: Specialized heads do the heavy lifting, the rest can be pruned. *arXiv preprint arXiv:1905.09418*, 2019.

Wang, K. R., Variengien, A., Conmy, A., Shlegeris, B., and Steinhardt, J. Interpretability in the wild: a circuit for indirect object identification in GPT-2 small. In *The Eleventh International Conference on Learning Representations*, 2023. URL <https://openreview.net/forum?id=NpsVSN6o4ul>.

Zaheer, M., Kottur, S., Ravanbakhsh, S., Poczos, B., Salakhutdinov, R. R., and Smola, A. J. Deep sets. In Guyon, I., Luxburg, U. V., Bengio, S., Wallach, H., Fergus, R., Vishwanathan, S., and Garnett, R. (eds.), *Advances in Neural Information Processing Systems*, volume 30. Curran Associates, Inc., 2017. URL <https://proceedings.neurips.cc/paper/2017/file/f22e4747dalaa27e363d86d40ff442fe-Paper.pdf>.

Zhai, X., Kolesnikov, A., Houlsby, N., and Beyer, L. Scaling vision transformers. In *Proceedings of the IEEE/CVF conference on computer vision and pattern recognition*, pp. 12104–12113, 2022.

A. Implementation details

Accompanying code may be found on [github](#).

All experiments are based on Vision Transformer (ViT) models implemented using the `timm` library. Unless otherwise stated, we use standard ViT architectures (e.g., patch size 16, image resolution 224) with modifications described below.

To study information-restricted attention, we wrap the attention module to bottleneck the per-head residual updates. For every head, the message passes through a variational information bottleneck (IB) module before being written to the residual stream. The IB is applied independently per attention head and per token, and returns both the transformed messages and a KL-divergence term used for regularization during training. For classification, we use global average pooling over the token representations and then apply the final projection to class logits. The remainder of the ViT architecture (patch embedding, positional embeddings, MLP blocks, normalization layers) follows the standard ViT design.

Optimization. Models are trained using the AdamW optimizer with a base learning rate of 6×10^{-4} and a weight decay of 0.05, for 1000 epochs. Bias parameters, parameters with dimensionality one (e.g., LayerNorm scale parameters), and all parameters in the IB encoder and decoder are excluded from weight decay. All other parameters, including patch embeddings and positional embeddings, are subject to weight decay. Automatic mixed precision (AMP) is used with gradient scaling.

Training uses a cosine learning-rate schedule with linear warmup over the first 10 epochs. The coefficient β is fixed over the course of training.

Data and Augmentation. Experiments are conducted on the 100-class subset of Imagenet used in [Tian et al. \(2020\)](#) and specified in the accompanying [github repository](#). Training images are augmented using random resized cropping, horizontal flipping, and RandAugment ([Cubuk et al., 2020](#)). We use a random resized crop with scale range [0.08, 1.0] and RandAugment with two augmentation operations of magnitude 9. Validation images are resized and center-cropped without stochastic augmentation. All images are normalized using standard ImageNet mean and standard deviation values.

B. Similarity of classification outputs between models in the spectrum

We compared the similarity of classification probability vectors for models across the spectrum, using the Jensen-Shannon divergence. The divergence values, grouped into five bins, are shown in Fig. 7.

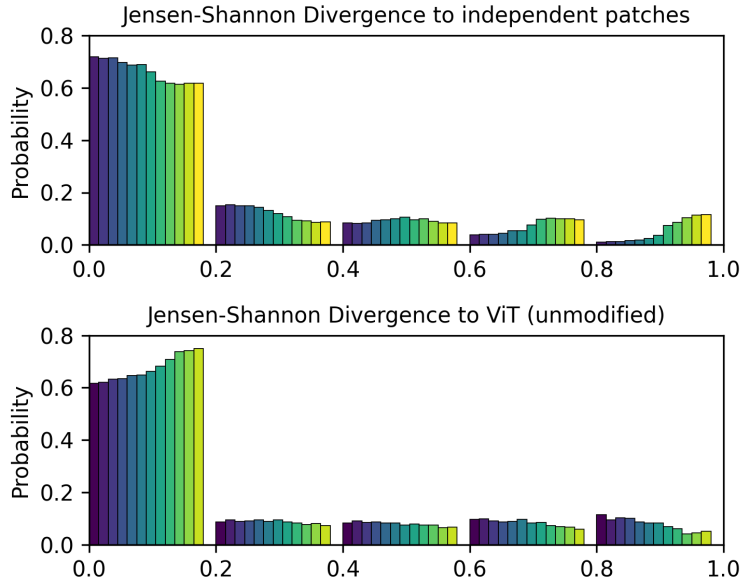


Figure 7. Jensen-Shannon divergence between classification outputs across the spectrum. For all images in the validation set, we measure the similarity of model classification outputs across the spectrum to that of the independent patch processing model (ViT w/o attention, dark blue, top row) and to that of the unmodified ViT (yellow, bottom row).

C. Additional comparisons between model updates and patch voting

In Figs. 8, 9, and 10, we show how different models along the spectrum “vote” for different images, and for the information restricted models, how the KL budget is spent.

D. Additional attention head highly activating patches

In Figs. 11&12, we show top activating patches of both polarities for other seeds at $\beta = 10$ and for the four active heads of the $\beta = 4$ model.

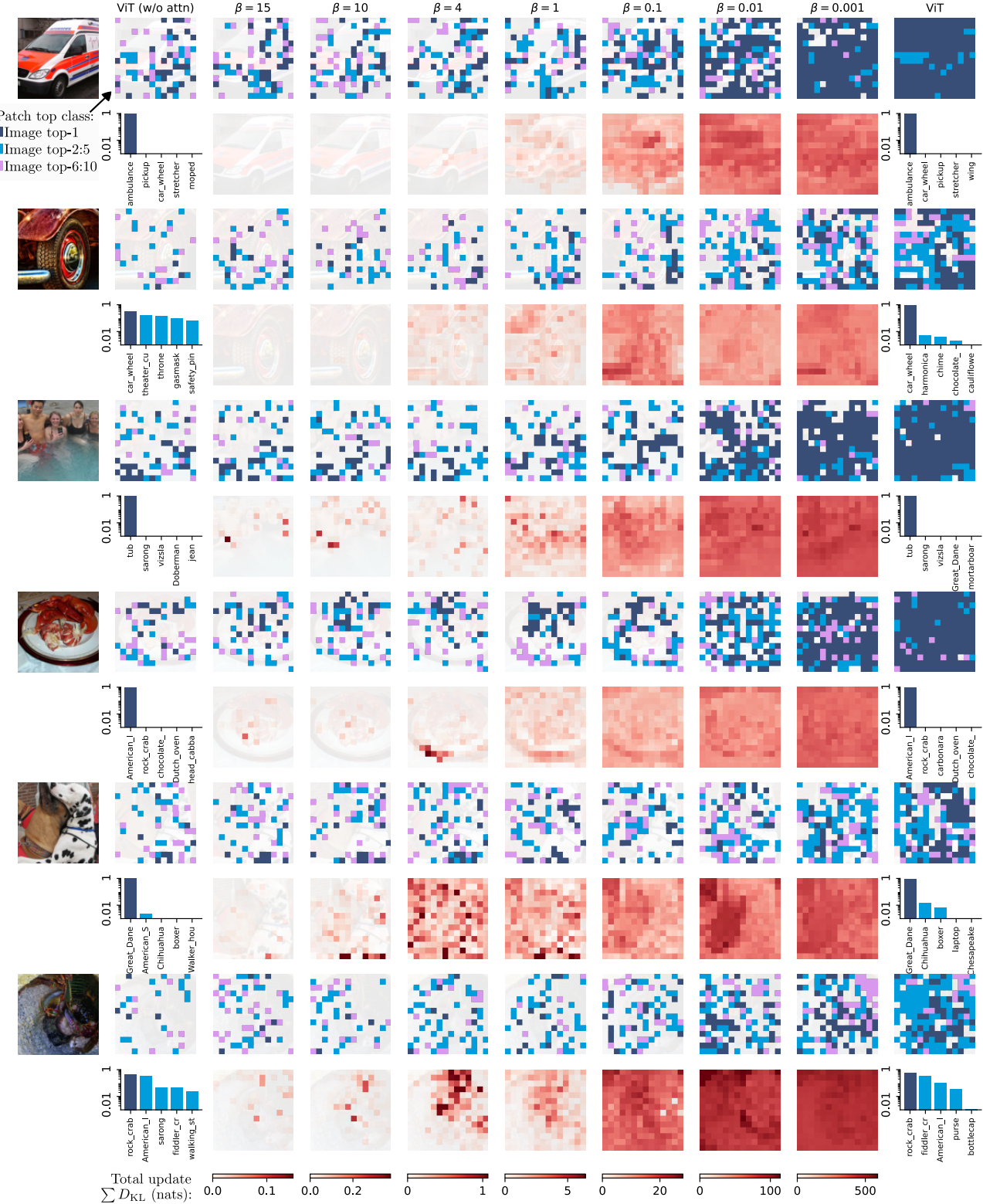


Figure 8. Patch voting and attention head update behavior for a random selection of images correctly classified by ViT (seed #1). Patches are colored according to the particular model's class assignments: dark blue for the patches whose top class matches that of the full image prediction top class, light blue for ranks 2 through 5, and pink for ranks 6 through 10.



Figure 9. Patch voting and attention head update behavior for a random selection of images correctly classified by ViT (seed #1) AND in the top 10% of images in terms of JSD between the ViT without attention and the unmodified ViT.

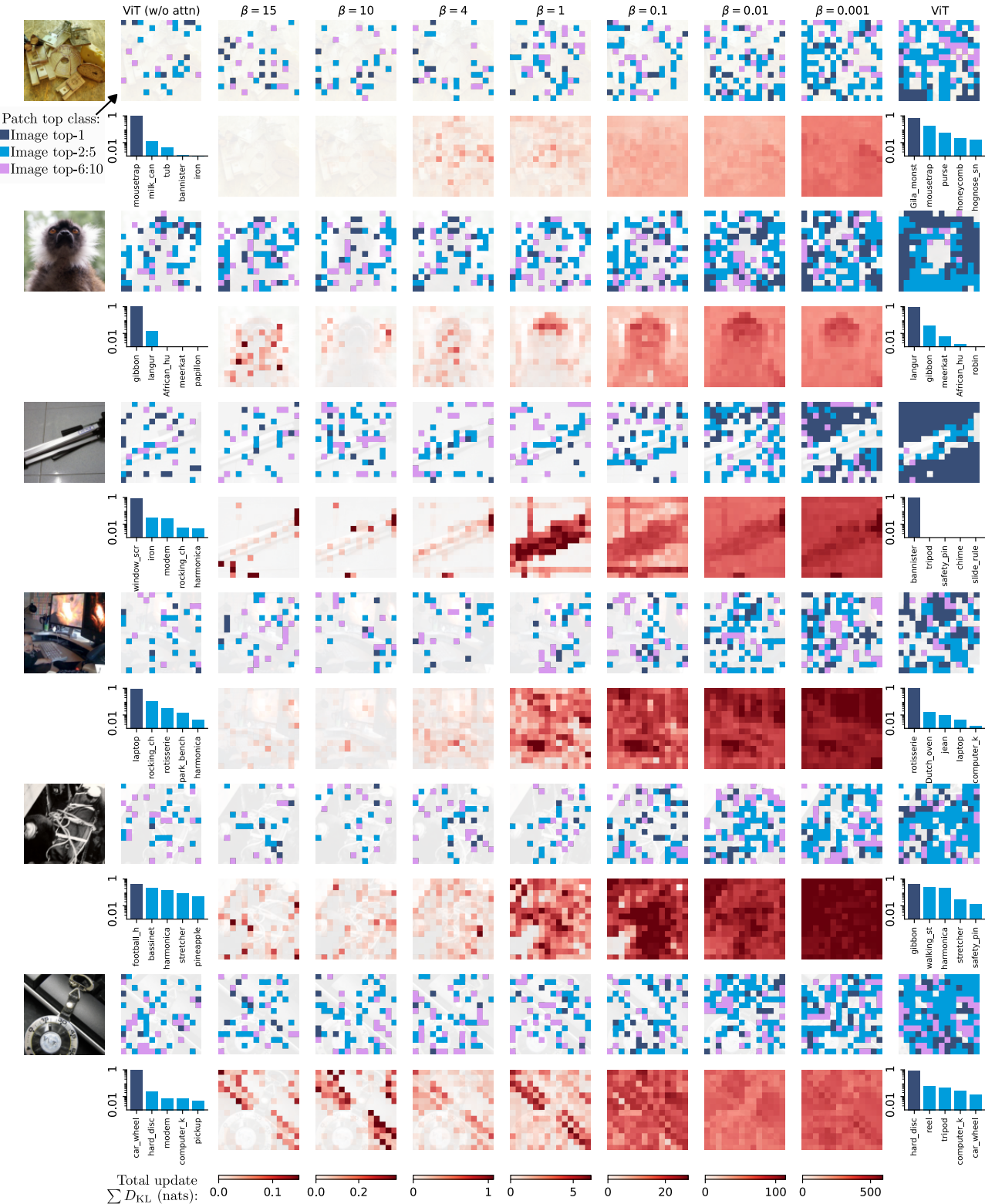


Figure 10. Patch voting and attention head update behavior for a random selection of images incorrectly classified by ViT (seed #1)

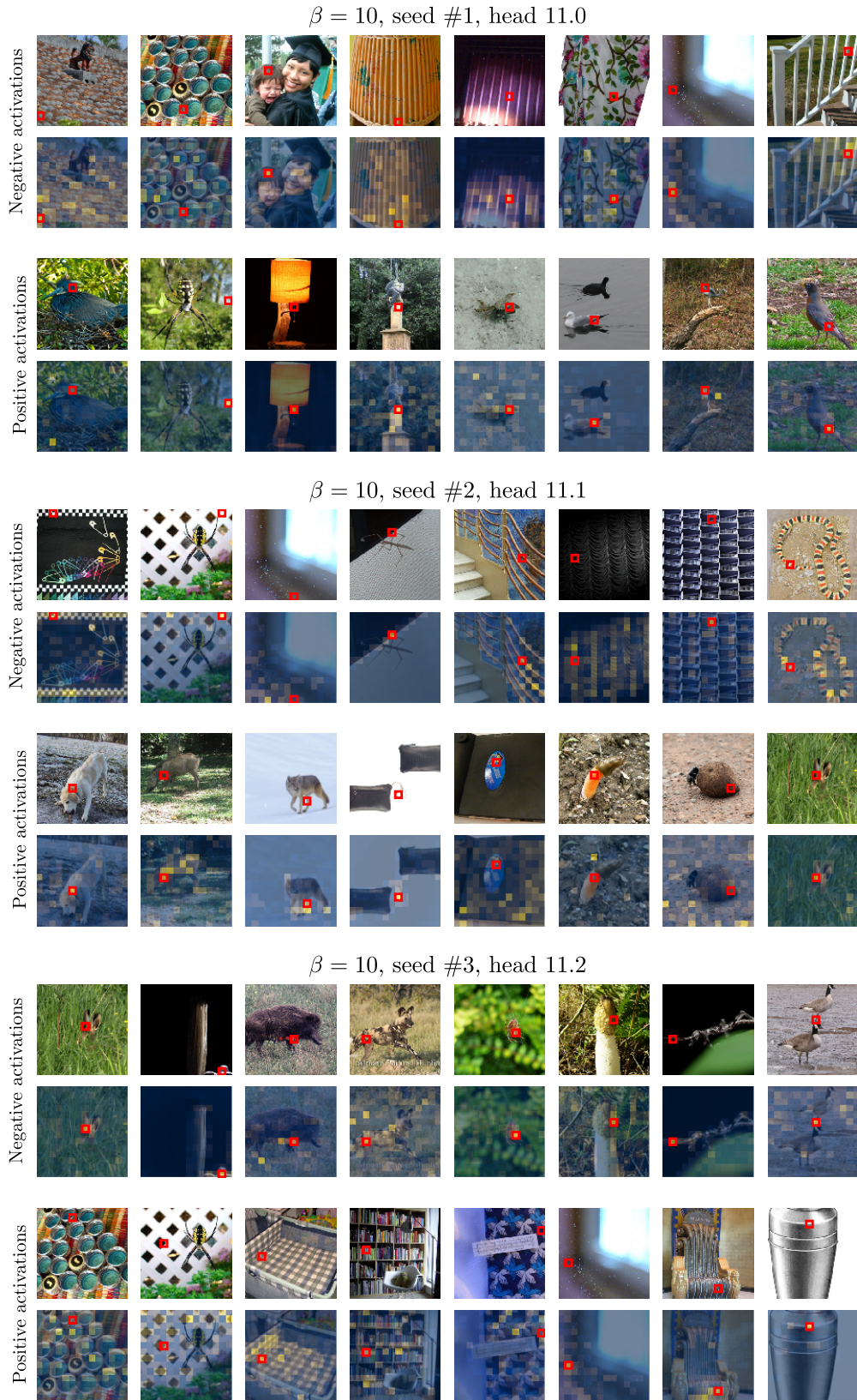


Figure 11. Additional top activation examples for heads with one active latent dimension: different $\beta = 10$ seeds.

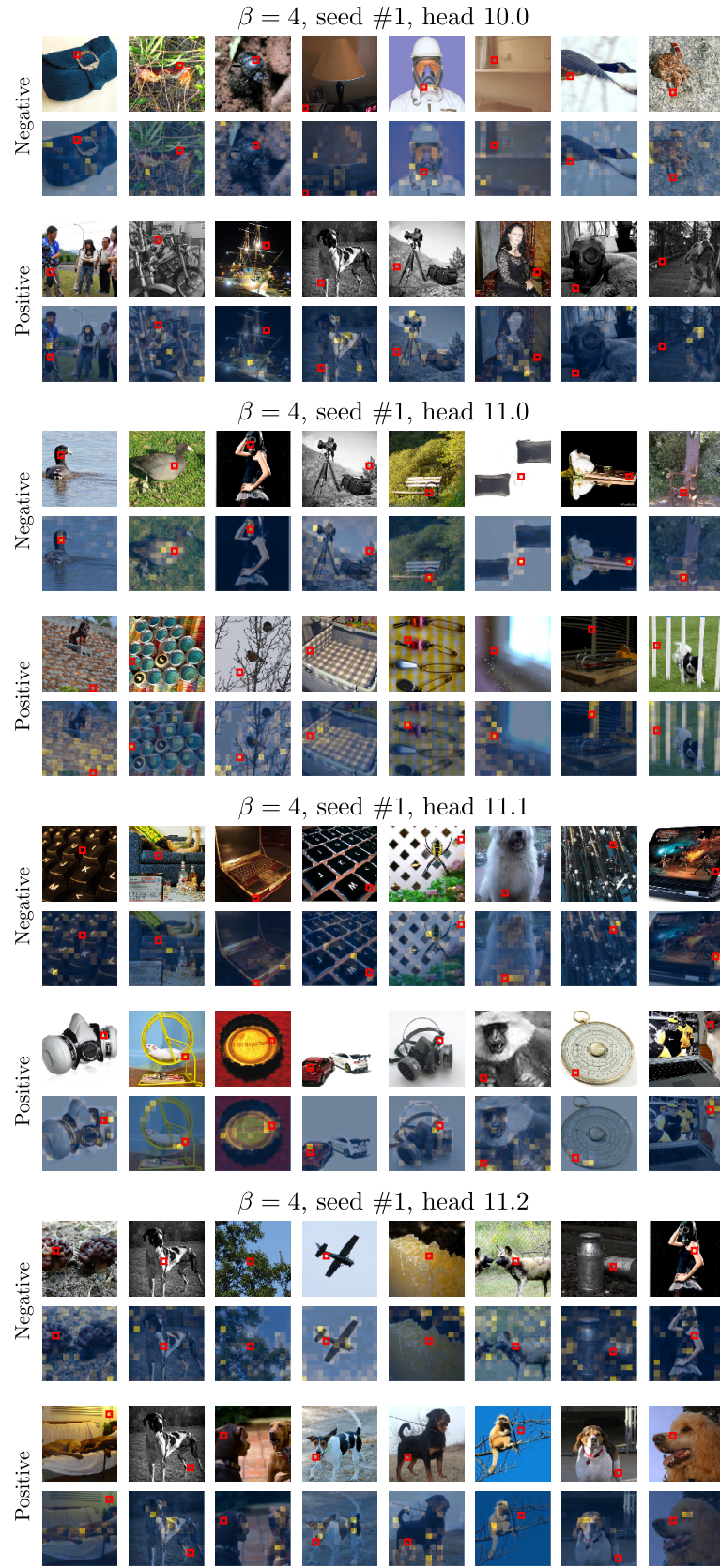


Figure 12. Additional top activation examples for heads with one active latent dimension: different heads in the $\beta = 4$ model.